meta-Benzyne Reacts as an Electrophile

Eric D. Nelson, Alexander Artau, Jason M. Price, Shane E. Tichy, Linhong Jing, and Hilkka I. Kenttämaa*

Department of Chemistry, 1393 Herbert C. Brown Lab. of Chemistry, Purdue University, West Lafayette, Indiana 47907-1393

Received: April 3, 2001; In Final Form: July 26, 2001

Examination of gas-phase reactions of various nucleophiles with *meta*-benzyne analogues that carry a positively charged substituent has revealed that the *meta*-benzyne moiety is susceptible to nucleophilic attack. Addition of nucleophiles to the *meta*-benzyne moiety occurs rapidly without energy-demanding uncoupling of the singlet biradicals' formally unpaired electrons. The resulting zwitterionic intermediate may undergo fragmentation either by a homolytic bond cleavage to yield net-radical type products or by a heterolytic bond cleavage that generally leads to replacement of the original charged group with the incoming nucleophile. The intermediate was characterized experimentally and computationally and found to be a low-energy species. The nonradical reactivity reported here is common for *meta*-benzynes with positively charged substituents, and is predicted also to dominate the chemistry of anionic and neutral *meta*-benzynes.

Introduction

meta-Benzyne, the middle child of the benzyne family, has not received the high degree of attention that has been lavished upon its *ortho*- and *para*-benzyne siblings. Difficulties in the generation and study of this interesting species have challenged the development of understanding of its reactivity. However, great strides have been made recently in a variety of avenues of research that provide information about the structure and thermochemistry of *meta*-benzyne. Threshold collision-activated dissociation (CAD) experiments have established its heat of formation,[1] and its singlet−triplet gap has been determined by negative ion photoelectron spectroscopy (NIPES) measurements.[2] These experiments and others have provided important experimental validation of the growing body of computational information regarding the structure and properties of *meta*-benzyne. Further information on its structure has been provided by matrix isolation[3] and NIPES[2] studies wherein its vibrational frequencies were measured. These frequencies were found to be more consistent with a diradicaloid (**1**) than a bicyclic (**2**) structure.

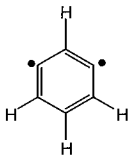

1

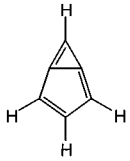

2

Yet, even though *meta*-benzyne is not bicyclic, the radical sites have a substantial degree of back-lobe interaction (clearly visible in the HOMO (right) and LUMO (left) of *meta*-benzyne, calculated at the BLYP/6-31+G(d) level of theory and shown on the right), resulting in a singlet ground state and a singlet−triplet gap of −21 kcal/mol.[2] Computational estimates further characterize it as possessing only 20% biradical character.[4] This species is thus often described as a combination of the two representations.[2,5]

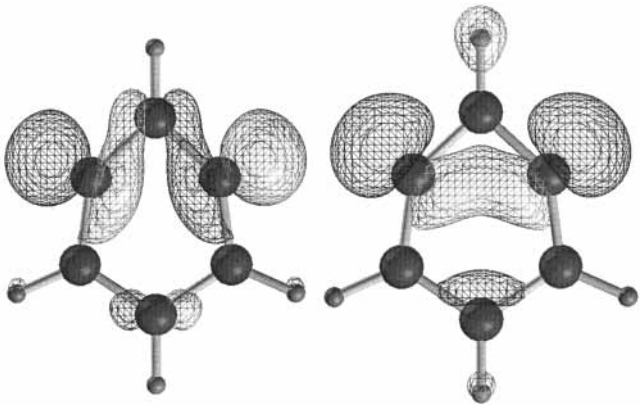

Despite successes in determining the structure and thermochemical properties of *meta*-benzyne, the characterization of its reactivity remains elusive.[5] The most successful approach at surmounting the difficulties inherent to any such study has been the examination of *meta*-benzyne analogues that bear a chemically inert, charged substituent. Such *meta*-benzynes have the virtue of being amenable to mass spectrometric analysis. The 3,5-didehydrobenzoate[6] (**3,** Scheme 1) and *N*-(3,5-didehydrophenyl)-3-fluoropyridinium[7] (**4**) ions have each been generated and their reactivity examined in the gas phase. Studies of these charged analogues represent the bulk of what is known about the chemical reactivity of the *meta*-benzyne moiety.

The 3,5-didehydrobenzoate ion (**3**) was found to be unreactive toward a number of neutral reagents that undergo radical reactions with the phenyl radical as well as its charged analogues.[6] In contrast, a wide variety of reactions were reported for the *N*-(3,5-didehydrophenyl)-3-fluoropyridinium ion (**4**), including several apparently free radical pathways.[7] This observation of free radical reactions contrasts with the lack of reactivity observed for **3**. Likewise, it contrasts with a recent paradigm of singlet biradical reactivity arising from studies of *para*-benzyne and its analogues.[8] This paradigm suggests that the radical-type reactivities of singlet biradicals can be seen as

10.1021/jp011254p CCC: $20.00
Published on Web 10/16/2001

SCHEME 1

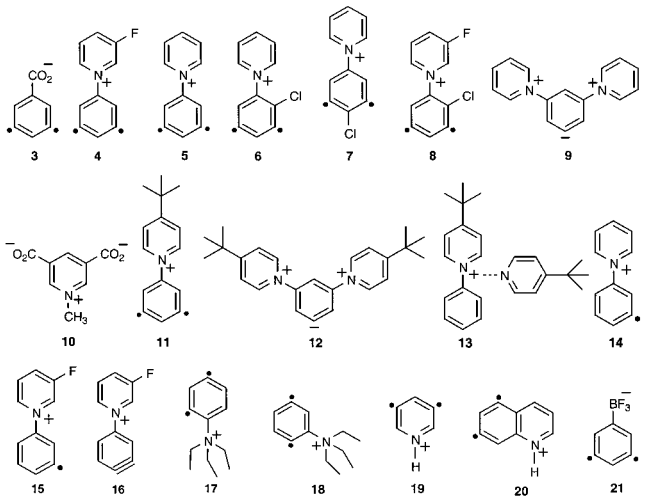

perturbed counterparts to the related monoradical reactivity. The perturbation takes the form of a decreased reactivity due to the singlet coupling between the biradical electrons. The singlet−triplet gap is used as an index of the degree to which the intrinsic radical-type reactivity is attenuated. Even a small singlet−triplet gap can have a large effect on the reactivity. For example, though *para*-arynes (i.e., 1,4-didehydrobenzene, 1,4-didehydronaphthalene, and 9,10-didehydroanthracene) undergo hydrogen atom abstraction from alcohols like the analogous aryl radicals, the rates of the abstractions are one to several orders of magnitude lower than those of their monoradical counterparts.[9,10] This decrease in reactivity has been attributed to *para*-benzyne's slight preference[2] for a singlet state ($\Delta E_{ST} = -3.8$ kcal/mol). In order for a free radical reaction to occur, the singlet pair of biradical electrons must uncouple in the course of the reaction,[11] imposing an extra energetic cost to the reaction. Although this may seem like a large inhibition to the reactions of singlet biradicals, it nevertheless should allow for faster reactions than a two-step mechanism in which intersystem crossing to the triplet state precedes reaction.

If *para*-benzyne's singlet ground state decreases the rates of its radical reactions by several orders of magnitude, then the corresponding decrease of *meta*-benzyne's reaction rates should be much greater due to this biradical's 5-fold larger preference for the singlet state.[12] If singlet−triplet gap effects on the reactions of singlet biradicals are in fact to be expected, then the apparent radical reactions of the *N*-(3,5-didehydrophenyl)-3-fluoropyridinium ion (**4**) are anomalously facile relative to those of corresponding monoradical ions.[7] For example, this *meta*-benzyne analogue undergoes cyano-radical abstraction from *tert*-butyl isocyanide at a rate only slightly (a factor of ∼5) less than that of the corresponding phenyl radical analogue.

Recently, we communicated the observation of a new type of electrophilic reactivity for several charged, substituted analogues of *meta*-benzyne.[13] This electrophilic reactivity provides an alternate interpretation of many of the previously observed "free radical" reactions, which removes the conflict with expectations[8,12] of decreased radical reactivity. We report herein a full description of this electrophilic reactivity.

Experimental Section

The majority of ion−molecule reactions were examined using a Fourier transform ion cyclotron resonance (FT-ICR) mass spectrometer. This instrument is an Extrel 2001 FTMS with a Finnigan Odyssey data station and extra inlets for the introduction of liquid and gaseous reagents into the ICR cell. Of special relevance to the current study is the fact that this instrument is one of a minority of FT-ICR's possessing a differentially pumped dual cell (i.e., a wall down the center of the vacuum chamber divides it into two nearly independent sections, each of which is pumped separately).[14] Ions can be transferred between the two cells by temporarily grounding the wall that separates the two cells (and serves as a common trap plate between them), thus allowing them to pass between the cells through a 2 mm diameter hole in the center of this wall. The efficiency of this transfer event is increased in many cases by the use of the quadrupolar axialization[15] technique prior to the transfer event. The experimental flexibility arising from the dual-cell instrumental configuration and the "tandem-in-time" nature of FT-ICR instruments allows multistep gas-phase syntheses for ions of interest and kinetic studies of their reactivities. In general, one of the two cells has been designated for ion generation and the other for kinetic studies of the resultant ions. Because reaction studies occur in a cell region that is differentially pumped with respect to the ion generation region, only very small amounts of the ion precursors are present. Thus, the reactions of the ions in the analysis region occur almost exclusively with the chemical species introduced purposely into this region for kinetic studies.

Charged *meta*-benzyne analogues were generated using one of two different methods. The first, which has been described previously,[7,16] involves the generation of substituted *N*-phenylpyridinium ions via an *ipso* substitution reaction between pyridine (or substituted analogues) and halobenzene radical cations (produced by electron ionization). The substituted *N*-phenylpyridinium ions are transferred into the other cell region. Collision-activated dissociation (CAD) of the *N*-phenylpyridinium ions homolytically cleaves the substituents (e.g., NO_2, I, Br) to form the *meta*-benzyne moiety.[17,18] A delay of ∼0.5 s after the CAD event allows the ions to dissipate any excess translational or internal energy by collisions with neutral molecules present in the cell and by emission of IR photons.[19] The ion of interest is isolated by ejection of all other ions from the cell with one or several stored-waveform inverse Fourier transform (SWIFT)[20] excitation pulses. The ions are then allowed to react with some neutral reagent of interest that is present in the ICR cell at a steady pressure. Variation of the time between the isolation of the *meta*-benzyne analogue and detection allows the ion population to react to different extents with the neutral reagent molecules. The resultant spectra were background corrected by subtraction of a spectrum collected under identical conditions except that the reactant ion was ejected via SWIFT excitation after isolation, but prior to the reaction time. Pseudo-first order reaction rate constants were extracted from a semilog plot of the relative abundances of the reactant and product ion abundances as a function of time. The measured rate constants were converted to second order rate constants (k_{rxn}) by dividing by the neutral reagent pressure. Typically, the measured second order reaction rate constants were on the order of 10^{-9} to 10^{-11} cm^3 molecule^{-1}s^{-1}. The measured rate constants were compared to the theoretical collision rate constants (k_{coll}) as predicted by the parametrized trajectory theory of Chesnavich and co-workers[21] to yield a reaction efficiency (i.e., $k_{rxn}/k_{coll}\ x\ 100$−the percent of collisions that result in reaction). The reaction efficiency was corrected for systematic errors in the nominal reagent pressure by a previously described method.[22] This method factors out errors in the pressure measurement for each neutral reagent with reference to ion−molecule reactions that are assumed to proceed

at the collision rate (e.g., exothermic electron transfer). The fastest such reaction is assumed to proceed at the collision rate and all other reaction efficiencies are normalized accordingly. Differences in relative abundances of the various product ions at short and long reaction times allow the assignment of primary and secondary products.

Slight deviations from the above procedures were made in studies of the 3,5-didehydrobenzoyl cation and the pyridine-substitution product of *N*-(2-chloro-3,5-didehydrophenyl)-3-fluoropyridinium ion. In the former case, it was the 3,5-dinitrobenzoyl cation (generated by EI of 3,5-dinitrobenzoyl chloride), rather than an *N*-phenylpyridinium ion, that was subjected to CAD to generate the ion of interest. In the latter case, CAD and subsequent ion−molecule reactions of the CAD product were performed *prior* to the transfer event, and it was the product of the fragment ion's reaction with pyridine that was transferred and whose reactions were examined in the other cell region.

The second method for the generation of *meta*-benzyne analogues in the FT-ICR relies on the charge-site substitution reactivity presented in this work (vide infra). Primary electron ionization (20 eV) of 3,5-dinitrobenzoyl chloride generates an abundant population of the 3,5-dinitrobenzoyl cation. Two sequential CAD events form the 3,5-didehydrobenzoyl cation. This ion was allowed to react with a neutral nucleophile to effect replacement of the CO moiety. The new *meta*-benzyne analogue was subsequently transferred into the second cell and allowed to react with a second neutral reagent, as described above. This method was used to generate all analogues described below, except those of the *N*-phenylpyridinium type.

Flowing-Afterglow Experiments. Characterization of the 3,5-bis(4-*tert*-butylpyridinium)phenide cation was conducted using a flowing-afterglow triple quadrupole apparatus, which has been described in depth previously.[23] The pressure and flow rate of the helium buffer gas in the 1 m × 7.3 cm (id) flow reactor were 0.4 Torr and 200 STP $cm^3\ s^{-1}$, respectively, with a bulk flow velocity of 9700 cm s^{-1}. The 3,5-bis(4-*tert*-butylpyridinium)phenide cation was generated via a slightly different synthesis procedure in the flowing-afterglow experiments than those described above for the FT-ICR due to the different capabilities of the two instruments. 3,5-Dinitroiodobenzene was introduced into the ion source region of the flow reactor and ionized to form the 3,5-didehydrophenyl cation (*m*/*z* 75).[24] This ion was transported by the flowing helium through the reactor, were it was allowed to react with 4-*tert*-butylpyridine to form the *N*-(3,5-didehydrophenyl)-4-*tert*-butylpyridium ion (*m*/*z* 210).[24] This ion was allowed to interact with a variety of reagents that have been shown previously to undergo characteristic reactions with the *N*-(3,5-didehydrophenyl)-3-fluoropyridium ion.[7] Observation of the previously reported reactivities of this ion demonstrated its presence in the flow tube. As in the FT-ICR, further reaction of the *N*-(3,5-didehydrophenyl)-4-*tert*-butylpyridium ion with 4-*tert*-butylpyridine results in the formation of the 3,5-bis(4-*tert*-butylpyridinium)phenide cation (*m*/*z* 345). A cluster ion between *N*-phenyl-4-*tert*-butylpyridinium ion and 4-*tert*-butylpyridine (*m*/*z* 347) was generated by primary electron ionization of chlorobenzene and reaction of the chlorobenzene radical cation with 4-*tert*-butylpyridine. The resultant *ipso*-substitution reaction that produces the *N*-phenyl-4-*tert*-butylpyridinium ion (*m*/*z* 212) is the same reaction that was used to generate substituted *N*-phenylpyridinium *meta*-benzyne precursors in the FT-ICR experiments (vide supra). Further reaction of this product ion (*m*/*z* 212) with 4-*tert*-butylpyridine results in the formation of small amounts of a cluster ion. Ions in the flowing afterglow plasma were thermalized to ambient temperature by ca. 10^5 collisions with the helium buffer gas. Positive ions were extracted from the flow reactor through a 0.5 mm orifice in a nose cone and focused into an Extrel triple quadrupole analyzer for mass spectrometric analysis.

CAD experiments were performed in the central, gas-tight collision chamber (Q2) of the triple quadrupole mass analyzer using argon (10−400 μTorr) as the target gas. The extraction lens voltage and the voltage bias of the third quadrupole (Q3) were adjusted to optimize product ion collection, and the Q3 mass resolution and other tuning conditions of the triple quadrupole analyzer were adjusted to achieve maximum reproducibility in the measurement of CAD cross sections. The collision energy was varied by changing the potential of Q2 relative to ground.

CAD Threshold Analysis. The data collection and analysis procedures used for CAD threshold measurements have been described in detail previously.[1,25] In these experiments, the yield of a particular CAD product ion is monitored while the axial kinetic energy of the reactant ion is varied. Product ion appearance curves are generated by plotting the CAD cross sections *vs* the reactant ion-target collision energy in the center-of-mass (cm) frame ($E_{cm} = E_{lab}[m/(M + m)]$, where E_{lab} is the lab-frame energy, m is the mass of the neutral target, and M is the mass of the reactant ion). Absolute cross sections, σ, for the formation of a single product by CAD are calculated using the thin-target expression,[26] $\sigma = I_p/Inl$, where I_p and I are the measured intensities of the product and reactant ion signals, n is the number density of the target gas, and l is the effective collision path length for reaction (24 ± 4 cm).[23] Phase incoherence between the quadrupolar fields in the individual quadrupoles of the triple quadrupole analyzer leads to oscillations in the apparent intensity of the reactant ion signal, but not the product signals, as the Q2 voltage is scanned. This variation of the signal during the scan is an artifact of the method and has no chemical significance. The "correct" behavior of the appearance curve is approximated by a best-fit step function in which the intensity of the ion signal in the oscillation region is assumed to be equal to the maximum intensity in the appearance curve prior to the onset of the intensity oscillation. This approximation does not affect the accuracy of modeling the threshold energies, since the portion of the appearance curve used for this purpose is typically free from intensity oscillations. However, it does result in an estimated factor of 2 uncertainty in determinations of absolute cross sections and ±20% uncertainties in the relative cross sections of different measurements.[23]

The threshold energies for dissociation are determined by fitting the product ion appearance curves with the model function given by eq 1, which takes into account the rovibrational contributions to the total available energy.[27]

$$\sigma = \sigma_0 \sum_{i=1}^{3n-6} P_D g_i (E_{cm} + E_i - E_0)^n / E \qquad (1)$$

In eq 1, E_o is the dissociation threshold energy, E_{cm} is the center-of-mass collision energy, σ_o is a scaling factor, n is an adjustable parameter, i denotes reactant ion vibrational states having energy E_i with a probability of occupation g_i ($\Sigma g_i = 1$), and P_D is the probability for dissociation of the ion at a given energy.

The appearance curves were modeled using the CRUNCH data analysis program written by Armentrout, Ervin, and coworkers.[26,28] The analysis utilizes an iterative procedure in which E_o, σ_o, and n are varied so as to minimize deviations between

the data and the calculated cross sections in the steeply rising portion of the threshold region. The center-of-mass collision energy, E_{cm}, is treated as a Gaussian energy distribution with a width of 1.5 eV (lab frame) at half-maximum to account for uncertainties. This kinetic energy uncertainty is further convoluted with a Doppler broadening function[29] to account for the random thermal motion of the target gas. The threshold energies obtained in this manner correspond to 0 K bond dissociation energies. The 298 K dissociation enthalpies are derived by combining the 0 K bond energy with the calculated difference in 0−298 K integrated heat capacities of the dissociation products and reactants, plus a PV work term ($RT = 0.6$ kcal/mol at 298 K). Finally, the cross section model shown in eq 1 explicitly accounts for the possibility of kinetic shifts by incorporating a probability factor, P_D, for the dissociation of the ion at a given energy. All threshold energies given are the average of three measurements conducted on different days.

Calculations. All theoretical energies reported in this study were calculated with the Gaussian 98 program.[30] Structures were fully optimized at the BLYP/6-31+G(d) level of theory. Each structure was verified to correspond to a stationary point on the BLYP/6-31+G(d) potential surface by vibrational frequency analysis (i.e., each structure possesses the correct number of imaginary frequencies−0 for minima, 1 for transition states). All energies include correction for the zero-point vibrational energy. The calculations of several potential energy surfaces as a function of a single specific bond length are an exception to the above. These energies are the result of a constrained partial optimization at the BLYP/6-31+G(d) level of theory in which a bond length was varied and its angle with respect to the rest of the molecule was held constant. All other variables were fully optimized. However, because these partially optimized structures are not stationary points on the potential energy surface, no vibrational frequency analysis was performed. The calculated electrostatic potential surface is the result of interaction of a positive point charge with the BLYP/6-31+G(d) wave function of the molecule over its surface (defined as electron density = 0.005 electrons/Å^3). The resultant range of energies is translated to a chromatic scale from red (lowest energy) to blue (highest energy) using Molden[31] for visualization. These surfaces thus provide a qualitative picture of the charge distribution in the molecule from red (most negative) to blue (most positive).

Results and Discussion

Previous speculation on the reactivity of *meta*-benzyne has centered on a proposal[12] of phenyl radical-type reactivity modified by the degree of singlet coupling between the biradical electron pair. As described above, the strong coupling between these biradical electrons may be expected to drastically attenuate the radical-type reactivity of this species. This would seem to make *meta*-benzyne fairly unreactive relative to the phenyl radical. However, this conclusion assumes that *meta*-benzyne can react only as a free radical. Our recent experimental results[13] suggest that this assumption is not valid for a large number of analogues of *meta*-benzyne bearing charged substituents. These species undergo rapid reactions that appear less inhibited than Chen's paradigm, based on the singlet coupling of the biradical pair, would suggest. These results thus provide a new paradigm of *meta*-benzyne reactivity to supplement the previous notions of weak radical-type reactivity.[12]

The most striking example of rapid, nonradical reactions by a charged *meta*-benzyne analogue can be found in the case of the 3,5-didehydrobenzoyl cation (Scheme 2). This species can be seen as a *meta*-benzyne with a positively charged acyl group located *meta* with respect to both radical sites. The 3,5-didehydrobenzoyl cation undergoes rapid reactions with many nucleophiles (e.g., tetrahydrofuran, dimethyl sulfide, trimethylphosphine, triethylamine, and pyridine) in which the nucleophile replaces the acylium charge site to generate a new *meta*-benzyne analogue (Table 1). For example, the 3,5-didehydrobenzoyl cation reacts with pyridine at 84% of the maximum possible rate (i.e., the collision rate) to form the *N*-(3,5-didehydrophenyl)-pyridinium ion (**5**) (Scheme 2a). The identity of this product ion was verified by generating the proposed ion via a CAD-based method reported previously[7] and comparing its reactivity (Figure 1a) to that of the substitution product (Figure 1b). The ions generated by these two methods react identically with *tert*-butyl isocyanide and in good agreement with previous studies[7] of the *N*-(3,5-didehydrophenyl)-3-fluoropyridinium ion.

SCHEME 2

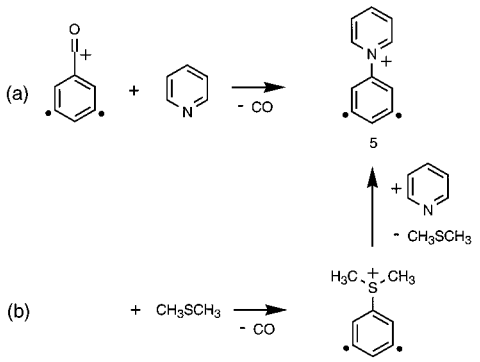

TABLE 1: Reactions of 3,5-Didehydrobenzoyl Cation with Selected Nucleophiles

nucleophile	proton affinity[a] (kcal/mol)	reactivity	reaction efficiency[b] (%)
water	166	no reaction	
methanol	180	no reaction	
ethanol	185	substitution[c]	0.08
propanol	188	substitution[d]	0.07[e]
dimethyl disulfide	194.9	substitution	25
tetrahydrofuran	196.5	substitution	21
dimethyl sulfide	198.6	substitution[c]	77
3-fluoropyridine	215.6	substitution	46
pyridine	222	substitution	84

[a] Proton affinity values from Reference 32. [b] Reaction efficiency is defined as the ratio of the measured second-order reaction rate constant to the theoretical collision rate constant x 100. [c] The product ion undergoes further reaction with the nucleophile. [d] Several other primary and secondary reactions were also observed. [e] This efficiency excludes all nonsubstitution reactivity.

The 3,5-didehydrobenzoyl cation is by no means the only *meta*-benzyne analogue to undergo the charge-site substitution reactivity. The new *meta*-benzyne analogues generated by the reactions of the 3,5-didehydrobenzoyl cation likewise undergo the charge-site substitution with nucleophiles to form new *meta*-benzyne analogues (Table 2). For example, when the product of reaction between the 3,5-didehydrobenzoyl cation and dimethyl sulfide was isolated and allowed to react with pyridine, an *N*-(3,5-didehydrophenyl)pyridinium product ion was formed that reacts (Scheme 2b, Figure 1c) in a manner identical to ions generated via the method of Reference 7 (Figure 1a). In fact, all the charge-substituted *meta*-benzyne analogues we have examined undergo charge-site substitution of some kind.

The observation of charge-site substitution is strongly correlated with the proton affinity (PA) of the incoming nucleophile

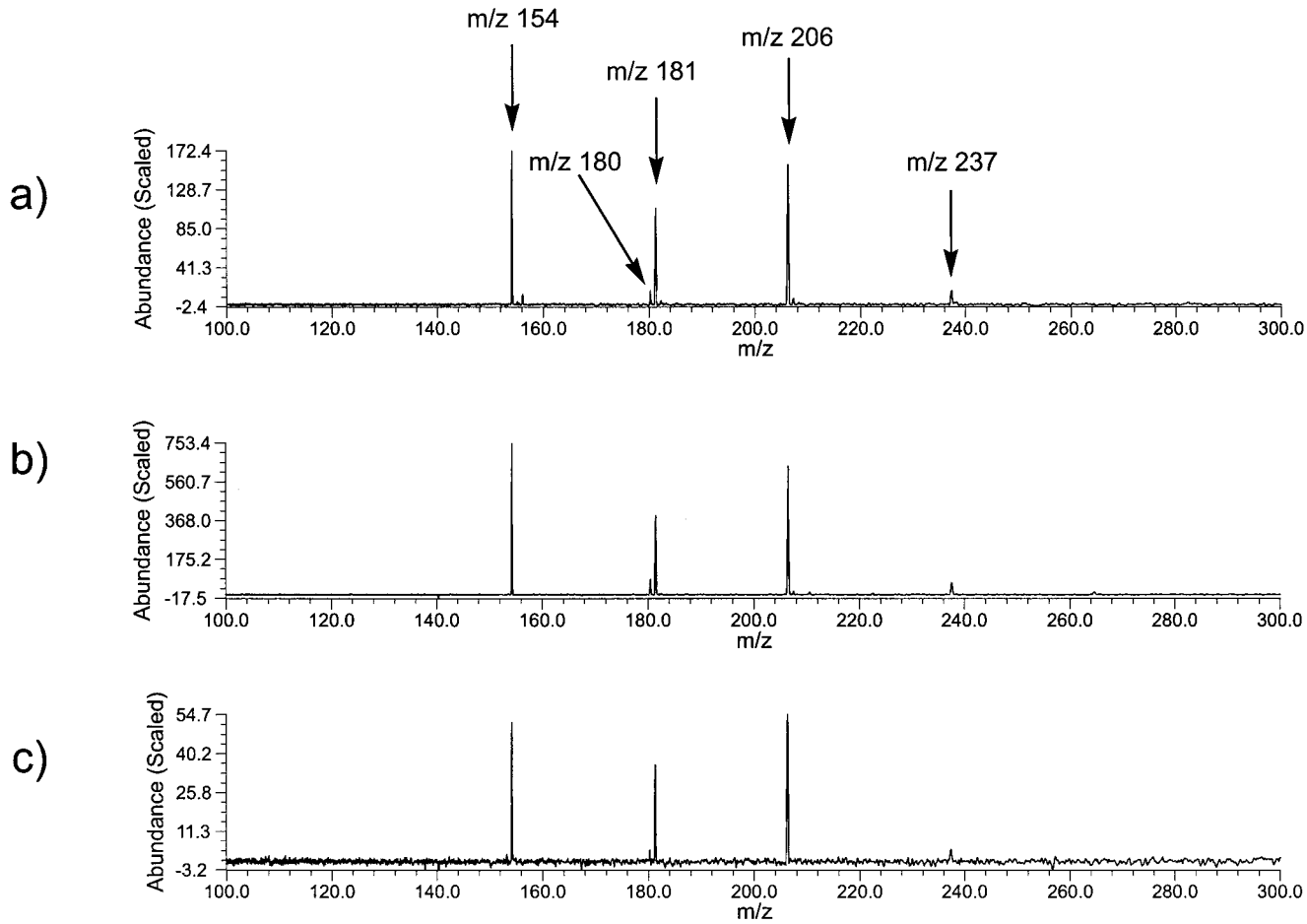

Figure 1. (a) Reaction of the *N*-(3,5-didehydrophenyl)pyridinium ion (*m*/*z* 154) for three seconds with *tert*-butyl isocyanide (1.2×10^{-7} Torr nominal pressure). The ion was generated from pyridine and 3,5-dibromonitrobenzene according to the method of Reference 7. Four characteristic reaction products are visible in the spectrum: M + CN (*m*/*z* 180), M + HCN (*m*/*z* 181), M + CN + CN (*m*/*z* 206) (a secondary reaction product of *m*/*z* 180), and M + *tert*-butyl isocyanide (i.e., adduct) (*m*/*z* 237). (b) Same reaction under the same conditions for *N*-(3,5-didehydrophenyl)-pyridinium ions generated by charge-site substitution of the 3,5-didehydrobenzoyl cation by pyridine. (c) Same conditions as in a and b, but the *N*-(3,5-didehydrophenyl)pyridinium ion was generated in two steps by reaction of the 3,5-didehydrobenzoyl cation with dimethyl sulfide and reaction of the resultant charge-site substitution product with pyridine.

TABLE 2: Substitution Reactions of Various *meta*-Benzyne Analogues

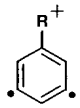

R=	PA (kcal/mol)[a]	nucleophile	PA (kcal/mol)[a]	reaction efficiency[b,c] (%)
tetrahydrofuran	196.5	dimethyl sulfide	198.6	4.5
dimethyl sulfide	198.6	*tert*-Butyl isocyanide	208.1	34
3-fluoropyridine	215.6	pyridine	222	2.0
3-fluoropyridine	215.6	3,5-dimethylpyridine	228.3	23
3-fluoropyridine	215.6	trimethylphosphine	229.2	37
pyridine	222	pyridine-d_5	222	0.4
pyridine-d_5	222	pyridine	222	0.4
pyridine	222	3,5-dimethylpyridine	228.3	21

[a] Proton affinity (PA) values from Reference 32. [b] Reaction efficiency is defined as the ratio of the measured second-order rate constant divided by the theoretical collision rate constant *x* 100. [c] Substitution was the only primary reaction in all cases.

and outgoing leaving group (Table 2). Typically, substitution was observed when the nucleophile is more basic than the leaving group. This observation is rationalized by the fact that the substitution reaction corresponds to the transfer of the 3,5-didehydrophenyl cation (a Lewis acid) between two bases. For example, the *N*-(3,5-didehydrophenyl)-3-fluoropyridinium ion (**4**) reacts with pyridine (PA = 222 kcal/mol *vs* 215.6 kcal/mol for 3-fluoropyridine[32]) to form the *N*-(3,5-didehydrophenyl)pyridinium ion (**5**), which in turn reacts with 3,5-dimethylpyridine (PA = 228.3 kcal/mol[32]) to form the *N*-(3,5-didehydrophenyl)-3,5-dimethylpyridinium ion. The reverse reactions were not observed due to their endothermic nature (~6 kcal/mol each at the BLYP/6-31+G(d) + ZPVE level of theory). Deviations from this basicity correlation occur in cases where either the reactant or the product charge site experiences resonance delocalization into the *meta*-benzyne ring. The 3,5-didehydrobenzoyl cation (Scheme 2) provides a good example of such deviations. The charge in this ion is resonance stabilized by delocalization with the phenyl ring. It is therefore less reactive than would be suggested by the low basicity of carbon monoxide (PA = 142 kcal/mol at the carbon[32]). For example, no substitution reaction is observed with water (PA = 165 kcal/mol[32]) or methanol (PA = 180.3 kcal/mol[32]), despite the fact that they are unquestionably more basic than CO (Table 1). The opposite situation occurs in the reaction of the *N*-(3,5-didehydrophenyl)-3-fluoropyridinium ion (**4**) with *tert*-butyl isocyanide. Although 3-fluoropyridine (PA = 215.6 kcal/mol[32]) is more basic than *tert*-butyl isocyanide (PA = 208.1 kcal/mol[32]), the *tert*-butyl isocyanidyl charge site experiences a benzylic resonance with the *meta*-benzyne ring that is not present for the

SCHEME 3

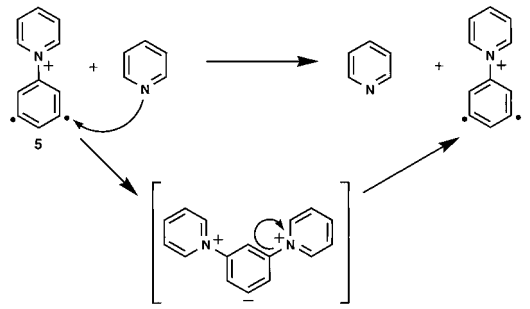

SCHEME 4

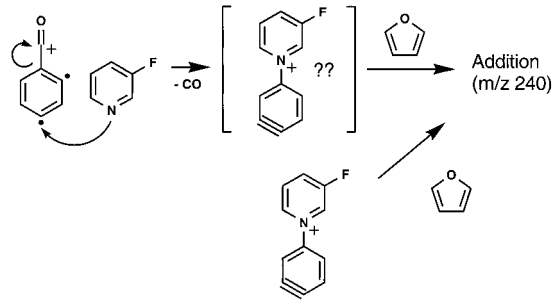

3-fluoropyridinium charge site. Thus, in this case, proton affinity is a poor predictor of the actual thermochemistry of the reaction.

Charge-site substitution depends on the presence of the *meta*-benzyne moiety and was not observed in its absence. For example, although substitution occurs between the 3,5-didehydrobenzoyl cation and most nucleophiles of PA greater than 180 kcal/mol, the benzoyl cation itself is unreactive toward most of these nucleophiles. This dependence of the substitution reactivity on the presence of the *meta*-benzyne moiety is inconsistent with a mechanism of *ipso*-substitution at the charge site. However, the net-*ipso*-substitution and importance of the *meta*-benzyne moiety can be reconciled by a mechanism of nucleophilic addition at the *meta*-benzyne moiety and elimination of the original charged moiety (Scheme 3). This can be seen to be the true nature of the substitution reactivity when the symmetry of the *meta*-benzyne analogue is broken to result in different products for *ipso*- and *meta*-attack. One example of this can be found in the 2,4-didehydrobenzoyl cation (Scheme 4). This species possesses the *meta*-benzyne moiety and was observed to undergo substitution with nucleophiles, just as the 3,5-didehydrobenzoyl cation. However, the products of such reactions display further reactivity that is characteristic of the presence of an *ortho*-benzyne rather than a *meta*-benzyne moiety (Scheme 4). For example, when this ion is reacted with pyridine, its substitution product undergoes further reaction by addition to furan and $HSCH_3$-abstraction from dimethyl disulfide—reactivities characteristic of the *N*-(3,4-didehydrophenyl)pyridinium ion (Scheme 4). The *N*-(2,4-didehydrophenyl)pyridinium ion (i.e., the product of *ipso*-substitution) is more than 600 times less reactive toward furan (although it also forms an adduct) and reacts with dimethyl disulfide by SCH_3 rather than $HSCH_3$ abstraction. The formation of *ortho*-benzyne isomers such as the *N*-(3,4-didehydrophenyl)pyridinium ion is the expected result if the initial attack occurs at the 4-position of this ion (i.e., at the *meta*-benzyne moiety).

A similar illustration of attack at the *meta*-benzyne moiety can be seen when the *meta*-benzyne ring is "labeled" with a chlorine substituent (Scheme 5). Though the products of *ipso*-substitution and *meta*-substitution are indistinguishable for an unlabeled *meta*-benzyne analogue such as **5**, its chloro-substituted isomers, the *N*-(2-chloro-3,5-didehydrophenyl)pyridinium (**6**) and *N*-(4-chloro-3,5-didehydrophenyl)pyridinium (**7**) ions, can be distinguished by their reactivity toward *tert*-butyl isocyanide. Although the 2-substituted ion reacts almost exclusively by HCN abstraction, the 4-substituted ion instead forms the *N*-(3-cyano-4,5-didehydrophenyl)pyridinium ion (a reaction channel involving the loss of chlorine) as the major product. When the *N*-(2-chloro-3,5-didehydrophenyl)-3-fluoropyridinium ion (**8**) undergoes substitution by a pyridine nucleophile, its substitution product displays reactivity toward *tert*-butyl isocyanide that is consistent with **7** rather than **6**, indicating that attack occurs preferentially at the 5-position (i.e., again at the *meta*-benzyne moiety).

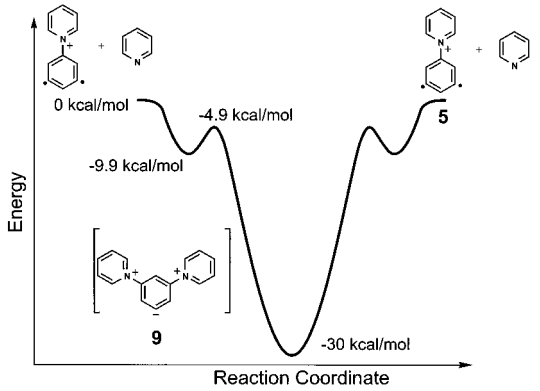

Figure 2. Potential energy surface calculated at the BLYP/6-31+G(d) + ZPVE level of theory for charge-site substitution of the *N*-(3,5-didehydrophenyl)pyridinium ion by pyridine.

SCHEME 5

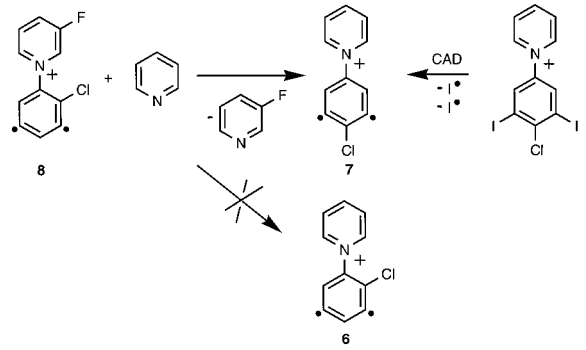

Calculations (BLYP/6-31+G(d)+ZPVE) suggest that the proposed addition−elimination mechanism of substitution (Scheme 3) is quite feasible. The predicted potential energy surface for the identity substitution in which a pyridine nucleophile replaces a pyridinium charged moiety is shown in Figure 2.

From this potential surface it can be seen that the nucleophilic addition occurs with only a moderate barrier (5 kcal/mol), and that the transition state actually lies 5 kcal/mol below the energy of the separated reactants (i.e., pyridine and the *N*-(3,5-didehydrophenyl)pyridinium ion) due to ion−molecule solvation.[33] Further, the intermediate implied in the mechanism (**9**) is quite stable, lying 30 kcal/mol below the reactants despite its unusual structure. This species has C_2 symmetry and a significant dipole moment of 9.8 D.[34] The calculated charge distribution of the intermediate (Figure 3) further bears out the predictions of charge separation implied by the Lewis structure shown in Figure 2. The graphical representation of the surface charge distribution in the intermediate (Figure 3) clearly shows that positive charge (blue) is distributed equally between the

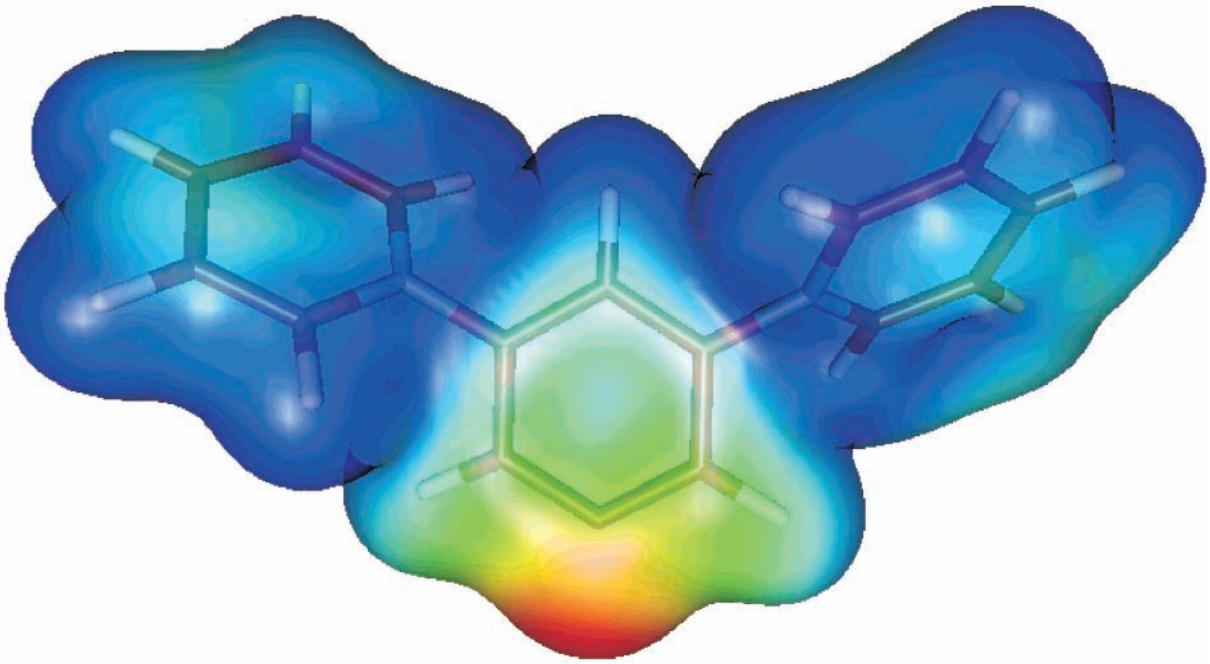

Figure 3. Electrostatic potential surface for the 3,5-bis-pyridiniumphenide cation calculated at the BLYP/6-31+G(d) level of theory. The graphic shown was calculated with Gaussian 98 and visualized with Molden. The illustration represents the interaction of a positive point charge with the surface of the BLYP wavefunction, with the resultant energies of interaction being graphed on a chromatic scale from red (lowest energy/most negative) to blue (highest energy/most positive).

two pyridinium moieties and that there is a localization of negative charge density (red) at the carbon bearing a negative formal charge in the Lewis structure. It is for this reason that we have chosen to name this species the 3,5-bis(pyridinium)-phenide cation.

The large degree of charge separation in the proposed intermediate clashes with intuition despite the calculated stability of this species. Certainly, spontaneous charge separation is not a common occurrence in the gas phase. Yet, there is some precedent for this type of species. For example, Beauchamp et al. have reported the intermediacy of salt-bridged structures in some H/D exchange reactions.[35] Others have reported evidence that certain peptide ions adopt salt-bridged structures as their preferred gas-phase isomers.[36] These salt-bridged ions benefit from strong Coulombic attraction between alternately charged moieties to mitigate the energetic cost of charge separation. More recently, the *N*-methylpyridinium-3,5-dicarboxylate anion (**10**) has been generated and found to be a stable structure in the gas phase, distinct from its isomers.[37] This latter species is quite analogous in relative charge orientation to the proposed 3,5-bis(pyridinium)phenide cation intermediate.

Precedent for the nucleophilic addition to singlet biradicals can be found in the generation of ylides by the reaction of singlet carbenes with nucleophiles.[38] The zwitterionic species formed by nucleophilic addition to the *meta*-benzyne moiety represent a greater amount of charge separation than ylides. However, these two reactions have in common the addition of a nucleophile to a singlet biradical species (this definition including carbenes in its broadest form) to form a charge-separated product.

Investigation of the 3,5-Bis(pyridinium)Phenide Cation Intermediate. The predicted stability of the 3,5-bis(pyridinium)-phenide cation (**9**) raises the possibility that it might be detectable under some conditions. Presumably, this intermediate possesses a lifetime of several hundred microseconds[39]—longer than the average collision complex, but too short for detection in the FT-ICR instrument. However, metastable species of this type may under certain circumstances undergo transition to long-term stability by the emission of IR photons[19] such that insufficient energy remains to allow dissociation to separated products. Such a transition to long-term stability is favored in the case of a thermoneutral substitution reaction and an intermediate that possesses a large number of vibrational modes, increasing the density of states (and thus the lifetime) of the intermediate and allowing increased number of pathways to IR emission. Such a case exists for the identity substitution reaction of the *N*-(3,5-didehydrophenyl)-4-*tert*-butylpyridinium (**11**) with 4-*tert*-butylpyridine. Substitution in this case results in no change in ion mass, and the experiment is blind to such reactivity. However, observation over long reaction times revealed the formation of a product of *m*/*z* 345, corresponding to the combined masses of **11** (*m*/*z* 210) and 4-*tert*-butylpyridine (MW 135). Figure 4 shows an example of one such reaction spectrum resulting from approximately 1400 ion−molecule collisions per ion[40] before the collection of the mass spectrum. These many encounters between the reactants presumably result in many identity substitutions and correspondingly large numbers of 3,5-bis(4-*tert*-butylpyridinium)phenide cation (**12**) intermediates. A small fraction of these intermediates is able to make the transition to long-term stability and mass spectrometric detectability. A similar (albeit slower) adduct formation was observed in the absence of the *tert*-butyl groups (i.e., for the reaction of the *N*-(3,5-didehydrophenyl)pyridinium ion (**5**) with pyridine to form the unsubstituted bis(pyridinium)phenide cation) (**9**). No addition was observed under the same conditions for related ions without a *meta*-benzyne moiety (e.g., the *N*-phenyl-4-*tert*-butylpyridinium and *N*-phenylpyridinium ions), suggesting that the observed adduct formation is not electrostatic clustering and that the addition is the result of reaction at the *meta*-benzyne moiety.

The chemical nature of the 3,5-bis(4-*tert*-butylpyridinium)-phenide cation (**12**) was examined in a flowing afterglow-triple-quadrupole apparatus. The collision-activated dissociation (CAD) threshold for loss of 4-*tert*-butylpyridine (the lowest energy

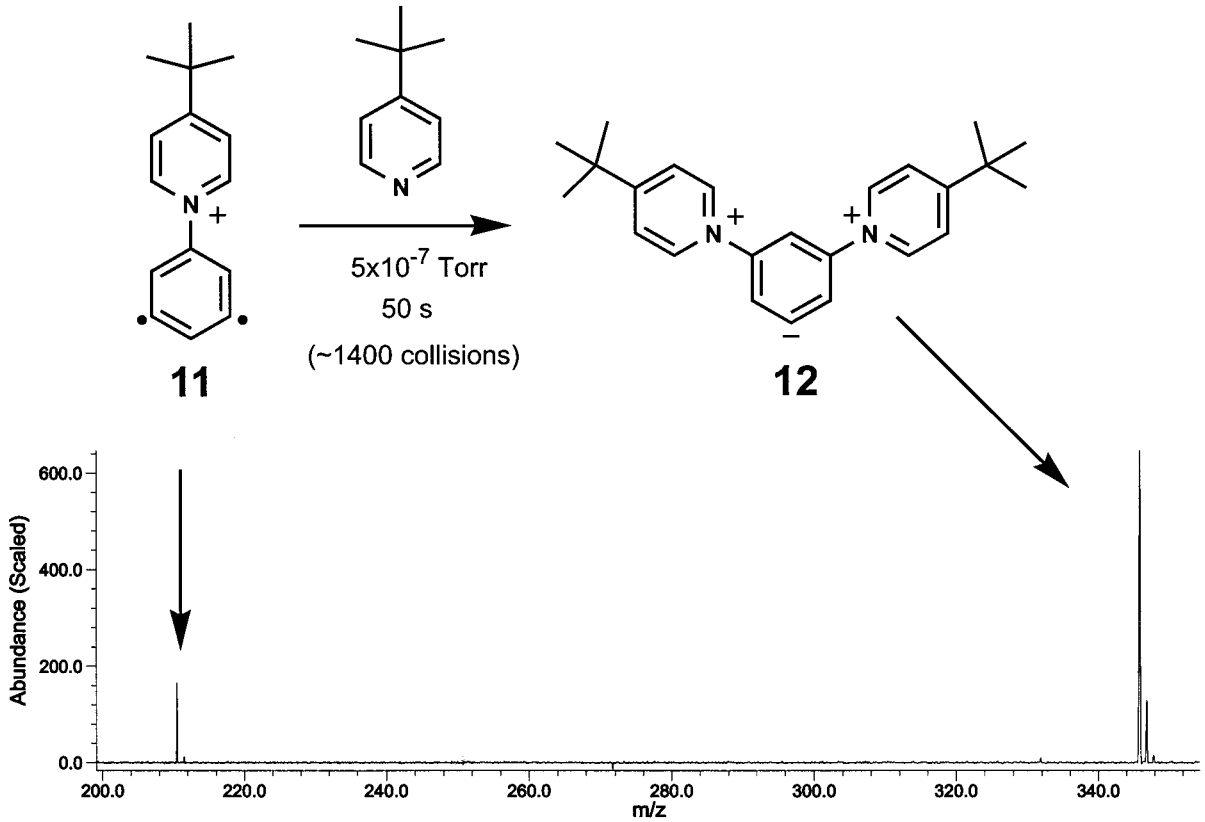

Figure 4. Reaction of the *N*-(3,5-didehydrophenyl)-4-*tert*-butylpyridinium ion (*m*/*z* 210) with 4-*tert*-butylpyridine (5.0×10^{-7} Torr nominal pressure) for 50 s to form the bis-(4-*tert*-butylpyridinium)phenide cation. The spectrum shown is the result of ~1400 collisions.

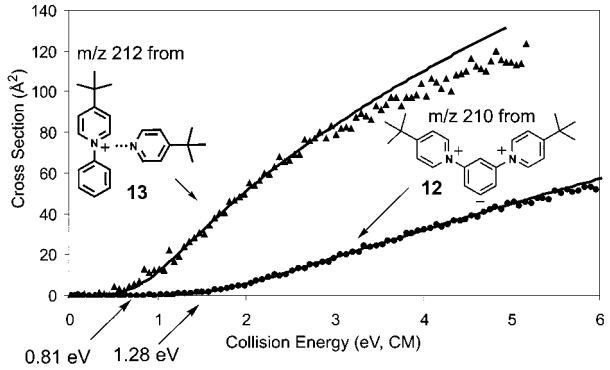

Figure 5. Separately measured cross sections for CAD of **12** and **13** as a function of center-of-mass collision energy. The loss of 4-*tert*-butylpyridine was monitored. The data were collected at various argon pressures and extrapolated to zero target gas pressure. The solid lines are fit to the data calculated by the method of Reference 28.

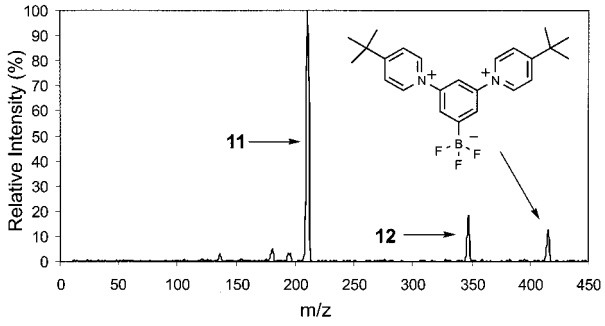

Figure 6. Reaction of the bis-(4-*tert*-butylpyridinium)phenide cation with BF_3 (3.0×10^{-5} Torr) in the central quadrupole of the flowing afterglow-triple quadrupole apparatus at a parent ion kinetic energy of −3 eV. An addition product (*m*/*z* 413) is observed in addition to CAD products (*m*/*z* 210, etc.).

fragmentation pathway) from this ion was measured to be 1.28 ± 0.16 eV (30 ± 4 kcal/mol). This value compares well with the 30 kcal/mol threshold calculated for the unsubstituted 3,5-bis(pyridinium)phenide cation species (**9**) (vide supra). It is also significantly larger than the 0.77 ± 0.09 eV (18 ± 2 kcal/mol) threshold measured for 4-*tert*-butylpyridine loss from the electrostatic cluster of the *N*-phenyl-4-*tert*-butylpyridinium ion and 4-*tert*-butylpyridine (**13**) (Figure 5). This clustered adduct forms much more slowly than **9**, but small amounts (<5% of *N*-phenyl-4-*tert*-butylpyridinium ion abundance) can be generated when 4-*tert*-butylpyridine pressure in the flow tube is maximized. This ion serves as a model of noncovalent association between the *N*-(3,5-didehydrophenyl)-4-*tert*-butylpyridinium ion (**11**) and 4-*tert*-butylpyridine. The significant difference in the threshold energies measured for these two related systems, and the close agreement of the former with *ab initio* calculations, strongly suggest that the nature of bonding in this species is weakly covalent, and that the 3,5-bis(4-*tert*-butylpyridinium)-phenide cation (**12**) is indeed the identity of the *m*/*z* 345 adduct ion.

The proposed 3,5-bis(4-*tert*-butylpyridinium)phenide cation (**12**) structure of the addition intermediate is further demonstrated by its ion−molecule reactivity. Although this ion bears a net positive charge, the localization of electron density at the phenide moiety allows it to react as a nucleophile in some cases. When the argon collision gas in the central quadrupole (Q2) of the flowing afterglow-triple quadrupole apparatus was replaced by the strong electrophile boron trifluoride and the collision energy was lowered, a new peak in the mass spectrum was observed that corresponds to the addition of BF_3 to the 3,5-bis(4-*tert*-butylpyridinium)phenide cation (**12**) (Figure 6).[41]

No reaction with BF_3 was observed for the *N*-(3,5-didehydrophenyl)-4-*tert*-butylpyridinium ion or the *N*-phenyl-4-*tert*-

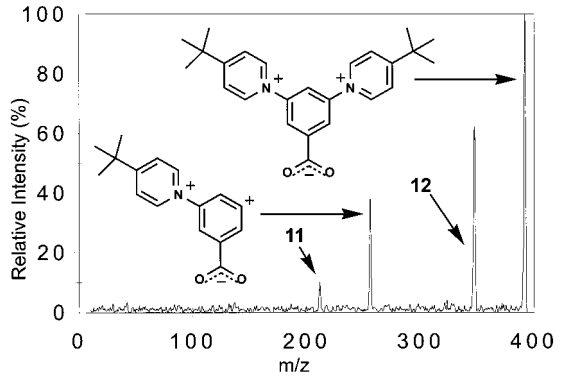

Figure 7. CAD of the CO_2 adduct of the bis-(4-*tert*-butylpyridinium)-phenide cation (*m*/*z* 389) in the flowing afterglow-triple quadrupole apparatus at a collision energy of 20 eV lab (1.86 eV center-of-mass) and argon target gas pressure of 1×10^{-4} Torr. Product ions include *m*/*z* 345 (loss of CO_2), *m*/*z* 254 (loss of 4-*tert*-butylpyridine), and *m*/*z* 210 (loss of both CO_2 and 4-*tert*-butylpyridine).

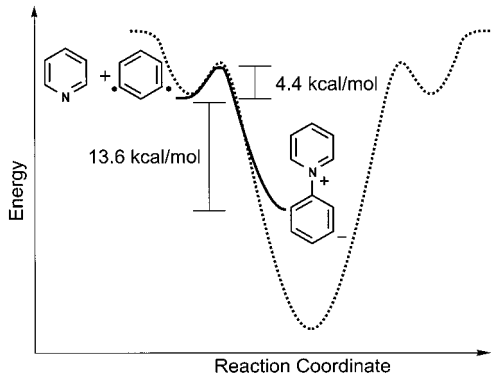

Figure 8. Potential energy surface calculated at the BLYP/6-31+G-(d) + ZPVE level of theory for the addition of pyridine to *meta*-benzyne. The potential energy surface for the addition of pyridine to the *N*-(3,5-didehydrophenyl)pyridinium ion (Figure 2) is overlaid for comparison.

butylpyridinium ion/4-*tert*-butylpyridine cluster under similar conditions.

The BF_3-addition reaction is mirrored in a similar, albeit slower, addition reaction that was observed to occur between the 3,5-bis(4-*tert*-butylpyridinium)phenide cation (**12**) and carbon dioxide (CO_2) in the flow tube. CAD of this CO_2 adduct results in the losses of CO_2 and/or 4-*tert*-butylpyridine from the parent ion (Figure 7). The competitive dissociation behavior supports a covalently bound structure for the CO_2 adduct. Analogous CO_2 and BF_3 addition reactivities have been reported for many gas-phase anions, including phenide.[42] They are, however, very unusual reactivities for a positive ion, and thus quite characteristic of the 3,5-bis(pyridinium)phenide structure.

Kinetic Aspects of the Substitution Reactivity. Although a nucleophilic charge-site substitution was observed for a wide variety of charged *meta*-benzyne analogues, the rates of these substitution reactions vary widely (Table 2). This arises from the presence of small, but kinetically significant, barriers to nucleophilic addition. For example, the identity substitution reaction in which pyridine replaces a pyridinium charge site (shown in Figure 2) occurs in only one out of ~200 collisions.[43] In the absence of any barrier to the nucleophilic addition step, the reaction would be expected to proceed in one out of every two collisions due to the equivalence of reactants and products. Thus, the present case of nucleophilic charge-site substitution appears to possess a 100-fold rate decrease relative to this barrierless reaction ideal that arises from a moderate (~5 kcal/mol) barrier to the addition step (Figure 2).

Nucleophilic addition to the *meta*-benzyne moiety appears to be fundamental to this moiety and only slightly perturbed by the presence of the charged moiety. For example, the potential energy surfaces for the nucleophilic addition of pyridine to neutral *meta*-benzyne (Figure 8) and its analogue, the *N*-(3,5-didehydrophenyl)pyridinium ion (**5**) (Figure 2), are qualitatively similar (i.e., addition with a moderate barrier to form a lower energy zwitterionic adduct). The only substantial difference between the two potential energy surfaces is the presence of an ion−molecule solvation well[33] and a greater exothermicity in the case of the charged analogue. The increased exothermicity of the reaction of the charged analogue relative to *meta*-benzyne itself can be understood from a purely electrostatic perspective as the stabilizing interaction of an ion (the pyridinium charged moiety present in the reactant ion) with a strong dipole (the pyridinium phenide moiety resulting from the addition of pyridine to *meta*-benzyne). This ion−dipole

SCHEME 6

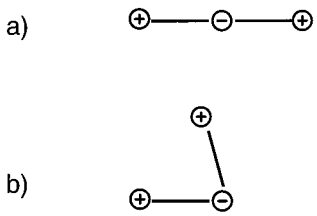

SCHEME 7

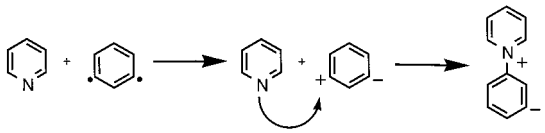

stabilization effect is incomplete due to the nonoptimal orientation of the pyridinium phenide dipole and the pyridinium charged moiety (i.e., an angle of ~80° rather than the preferred 180°; Scheme 6).[44] If the geometry of the adduct were loose enough to allow the relaxation of the ion−dipole angle to the ideal 180°, this would result in the formation of a salt-bridged structure similar to those observed previously by Beauchamp et al.[35]

The barrier that accompanies addition of pyridine to *meta*-benzyne (Figure 8) can be thought of as the result of an avoided crossing between the stabilizing potential of bond formation and destabilizing potential of charge separation as a nucleophile approaches *meta*-benzyne (Scheme 7). An illustration of this avoided crossing is shown in Figure 9. This depiction of the origin of the addition barrier is essentially a valence bond curve-crossing model similar in spirit to those described by Shaik et al.[45] Such models provide qualitative insight into the factors that affect the origin of the chemical barrier by comparing the energies of the most important reactant and product valence states as a function of the reaction coordinate. Molecular orbital calculations can be used to estimate the energies of the valence states of interest. In the present case, the reaction coordinate corresponds essentially to the approach of the pyridine nitrogen to one of the radical sites of *meta*-benzyne, and the position along the reaction coordinate is indicated by the C−N bond length. The bond formation surface is modeled in Figure 9 by the bond formation between pyridine and the phenyl cation.[46] The charge separation surface is modeled by the polarization of *meta*-benzyne's biradical electron pair, induced by the approach of a neon atom to one of its radical sites.[47] Despite the crudity of this model, examination of Figure 9 reveals that

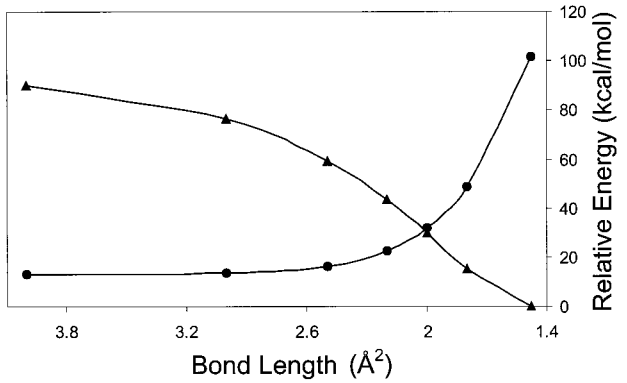

Figure 9. Depiction of the contributions of bond formation and charge separation to the barrier for pyridine addition to *meta*-benzyne. The bond formation potential (▲) is approximated by the bond formation between pyridine and the phenyl cation. The charge separation potential (●) is approximated by the polarization of *meta*-benzyne by the approach of a neon atom. All energies are calculated at the BLYP/6-31+G(d) level of theory.

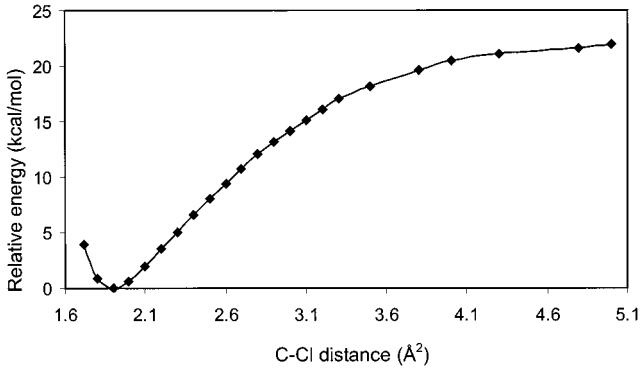

Figure 10. BLYP/6-31+G(d) potential surface for chloride addition to *meta*-benzyne to form 3-chlorophenide as a function of C−Cl bond distance.

the point of intersection between the two surfaces is only slightly (∼0.1 Å) offset from the transition state C−N distance of 2.158 Å calculated at the BLYP/6-31+G(d) level of theory.

A key test for the above avoided crossing model of the addition barrier may be found in the case of addition of anionic nucleophiles to *meta*-benzyne. Such addition reactions should entail no charge separation along the reaction coordinate, because the polarization of the *meta*-benzyne moiety is counterbalanced by the neutralization of the anionic nucleophile. Thus, the phenide moiety is formed in a transfer of charge from the nucleophile rather than a separation of charge at the *meta*-benzyne moiety, and no positive charge develops at any stage of the reaction. The loss of the repulsive charge-separation aspect of the addition reaction should allow addition to occur with small or negligible barrier. In fact, no barrier was found to accompany the addition of chloride to *meta*-benzyne at the BLYP/6-31+G(d) level of theory (Figure 10).[48] On the basis of this loss of the chemical barrier, it appears that anionic nucleophiles should show high affinity for nucleophilic addition to the *meta*-benzyne moiety, although this prediction cannot be tested with the mass spectrometric methods used in this study.

The efficiencies of charge-site substitution reactions are subject to significant changes with variation of the charged moiety of the *meta*-benzyne analogue. This contrasts sharply with the reaction efficiencies of charged phenyl radical analogues, whose reactions have been shown to be only moderately sensitive to the chemical nature of the charged moiety.[16c] For example, where the reactions of the phenyl radical analogues

SCHEME 8

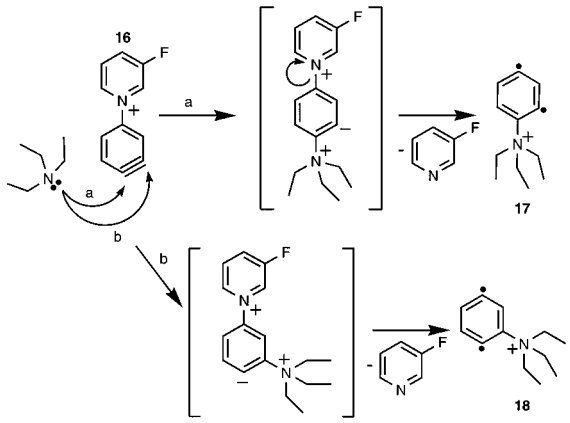

(e.g., the *N*-(3-dehydrophenyl)pyridinium (**14**) and *N*-(3-dehydrophenyl)-3-fluoropyridinium (**15**) ions) are almost identical for most neutral reagents (i.e., comparable products and reaction efficiencies), the equivalent *meta*-benzyne analogues, the *N*-(3,5-didehydrophenyl)-3-fluoropyridinium (**4**) and *N*-(3,5-didehydrophenyl)pyridinium (**5**) ions, show substantial differences in their reactions. For example, the net-substitution reaction with a pyridine nucleophile occurs five times faster for **4** than for **5** (2% *vs.* 0.4% efficiency, Table 2). Substitution on the *meta*-benzyne ring also has profound effects on the reaction kinetics. For example, the replacement of pyridine-d_5 by pyridine is accelerated by a factor of ∼30 when a chloro- or bromo-substituent is placed *ortho* with respect to the pyridinium charge site (∼13% *vs.* 0.4%). This rate enhancement is much greater than the factor of 2 rate enhancement resulting from chloro-substitution of the monoradical analogue **14**.[49] It is likely that the large substituent effects observed for the *meta*-benzyne analogues are a result of bond dipole and substituent polarizability effects on the stabilization of the zwitterionic transition states and reaction intermediates.

Related *ortho*-Benzyne Reactivity

Although *ortho*-benzyne is best known for its electrocyclic reactivity,[50] it is also quite reactive toward many reagents that do not contain double bonds. In some cases, the mechanisms proposed for these reactions involve *ortho*-benzyne acting as an electrophile.[51] Thus, it should not come as a surprise that the observed charged moiety substitution of *meta*-benzyne analogues is mirrored in the reactivity of the corresponding charge-substituted *ortho*-benzyne analogues. For example, the *N*-(3,4-didehydrophenyl)-3-fluoropyridinium ion (**16**) reacts with triethylamine by substitution and addition (i.e., the formation of a stable adduct) as its two major pathways of reaction.[7] Yet, because **16** lacks the symmetry of the *meta*-benzyne-type species shown in Scheme 3, addition and subsequent elimination necessarily result in the formation of a *meta*- or *para*-benzyne, rather than an *ortho*-benzyne product (Scheme 8).

The identity of the product is determined by the site of addition. Attack at the 4-postion by triethylamine (Pathway a; Scheme 8) results in the formation of the *N*-(2,4-didehydrophenyl)triethylammonium ion (**17**), a *meta*-benzyne analogue. Alternate attack at the 3-position (Pathway b; Scheme 8) results in the formation of the *N*-(2,5-didehydrophenyl)triethylammonium ion (**18**), a *para*-benzyne analogue. Because the neutral *meta*- and *para*-benzynes are significantly (16 and 31 kcal/mol,[1] respectively) higher in energy than *ortho*-benzyne, the reaction of the charged analogues can be expected to be intrinsically endothermic. To make the reaction exothermic, the nucleophile must be significantly more basic than the leaving group to make

SCHEME 9

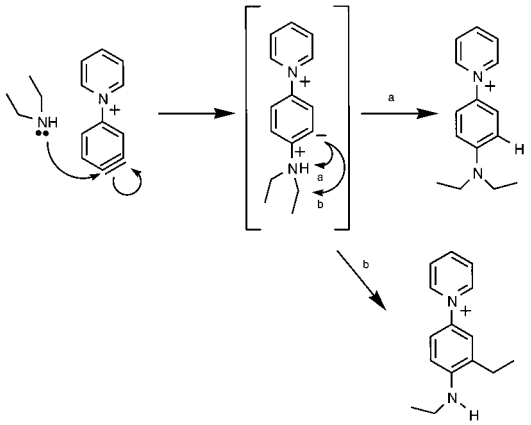

up for the loss of the inherent stability of the *ortho*-benzyne moiety. On the basis of the measured heats of formation of the neutral *meta*- and *para*-benzyne,[1] the first pathway (Scheme 8a) should be favored by about 15 kcal/mol over the second (i.e., by the relative energy difference between *meta*- and *para*-benzyne). Also, the addition intermediate leading to **17** (shown in the brackets in Scheme 8) is calculated to be 7 kcal/mol lower in energy than the intermediate leading to **18**,[52] further favoring the formation of **17** over **18**. Both *ortho*-benzyne intermediates are lower in energy (12 and 5 kcal/mol, respectively) than the *meta*-benzyne intermediate **9**. This can be explained on purely electrostatic grounds by a decreased degree of charge separation of both *ortho*-benzyne intermediates relative to **9**.[52] The lower energy intermediates and less exothermic substitution pathways translate to a longer intermediate lifetime, and the addition intermediate is often observed as a major product of the reactions of **16**. When substitution is endothermic (e.g., in the reaction of the *N*-(3,4-didehydrophenyl)pyridinium ion with pyridine-d_5), addition is usually the only reaction that is observed.

Unlike the addition intermediate of *meta*-benzyne analogues, the addition intermediates of *ortho*-benzyne analogues inherently possess a phenide moiety next to the new positively charged moiety. This is a situation that cries out for isomerization to transform the intermediate into a more stable form with significantly reduced charge separation. The reaction of diethylamine with the *N*-(3,4-didehydrophenyl)pyridinium ion provides a good example of such a situation. The addition intermediate in this reaction has two fairly facile isomerization pathways available to it: proton transfer and ethyl cation transfer by an S_N2 mechanism (Scheme 9). Both pathways are driven by stability of the resultant products, which do not possess the charge separation of the intermediate. CAD of this adduct proceeds mainly by loss of C_2H_6N (i.e., retention of one ethyl group from the eliminated triethylammonium moiety), suggesting that this second rearrangement pathway occurs during or prior to CAD. A similar retention of one ethyl group in the product ion is observed upon CAD of the addition product with triethylamine. This apparent rearrangement of the di- and triethylamine addition intermediates contrasts with the behavior of the pyridine-d_5 adduct with this same ion. Unlike the di- and triethylamine adducts, CAD of the pyridine-d_5 adduct results primarily in the loss of one of the two pyridine moieties, indicating the lack of isomerization pathways for this latter species.

Consequences of Addition Without Substitution. Although the above substitution reactivity is an important component of the reactivity of charged *meta*-benzyne analogues, it does not occur for all analogues of *meta*-benzyne. Certainly, although

SCHEME 10

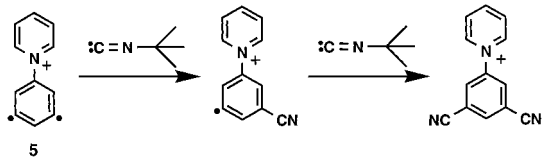

nucleophiles can add to *meta*-benzyne (Figure 8), it has no substituent to eliminate and cannot undergo substitution reactions. Likewise, not all charged *meta*-benzyne analogues undergo substitution. The examples range from species such as the 3,5-didehydropyridinium (**19**) and 5,7-didehydroquinolinium (**20**) ions, which do not have a leaving group on the ring, to the 3,5-didehydrophenyltrifluoroborate (**21**) and 3,5-didehydrobenzoate (**3**) ions whose charged moieties are negatively charged and cannot be replaced by nucleophilic addition.[53] Even those *meta*-benzyne analogues that *can* undergo substitution encounter many situations in which endothermicity prevents substitution. This is especially true for analogues whose charged moiety is a highly basic species (e.g., *N*-phenylpyridinium-type analogues). These analogues have in common with *meta*-benzyne itself the propensity for attack by nucleophiles without the reaction outlet of substitution. Because of this similarity, their reactions can be seen as models for the kinds of reactions that may occur as a consequence of nucleophilic attack on *meta*-benzyne. Several possible eventual fates for the addition intermediates include chemical reaction of the zwitterionic intermediates (e.g., nucleophilic reactivity observed for the 3,5-bis(4-*tert*-butylpyridinium)phenide cation), rearrangements (e.g., proton transfer between positive and negative charged moieties in the *ortho*-benzyne analogues), and fragmentation of the zwitterionic intermediate.

Fragmentation of the intermediate provides the especially interesting prospect of producing net-radical products via nonradical reaction steps. An example of one such reaction has been described in an earlier communication of this work.[13] The *N*-(3,5-didehydrophenyl)pyridinium ion (**5**) reacts with *tert*-butyl isocyanide by two sequential cyano-radical abstractions (among other pathways). This apparently free-radical reactivity corresponds qualitatively to *tert*-butyl isocyanide's reactivity toward free radicals in solution[54] and toward charged phenyl radical analogues in the gas-phase.[16c] Indeed, the second of the two CN abstractions undoubtedly is a free-radical process (Scheme 10). Yet, for the first abstraction to follow a free radical mechanism, the biradical electron pair must be uncoupled either before (i.e., intersystem crossing) or concerted with the reaction.[8,11] It has been suggested that the uncoupling of biradical electrons of such a singlet biradical in order to undergo radical-type reactivity has the effect of increasing the reaction barrier by a significant fraction (~2/3) of the singlet triplet gap of the biradical.[8] If this were to be the case for **5**, with its ~20 kcal/mol singlet−triplet gap,[55] it would result in radical-type reaction barriers being increased by more than 10 kcal/mol. Such large changes in the reaction barrier should slow this reaction by (at least) several orders of magnitude relative to the phenyl radical analogue (i.e., the *N*-(3-dehydrophenyl)pyridinium ion (**14**)).[56] Yet, the observed difference in the CN-abstraction rates of **5** and **14** is much less than this−only a factor of 5.[7] However, a mechanism of nucleophilic addition of *tert*-butyl isocyanide to the *meta*-benzyne moiety followed by fragmentation of the resulting adduct (Scheme 11) provides a route to the first CN-abstraction that is helped, rather than hindered, by the singlet ground state of *meta*-benzyne. *tert*-Butyl isocyanide is a moderately basic nucleophile (PA = 208 kcal/mol[32]) that is

SCHEME 11

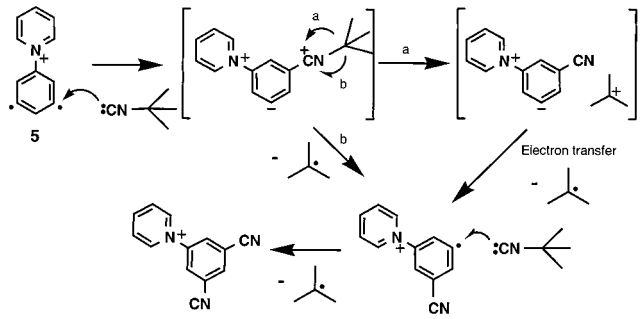

SCHEME 12

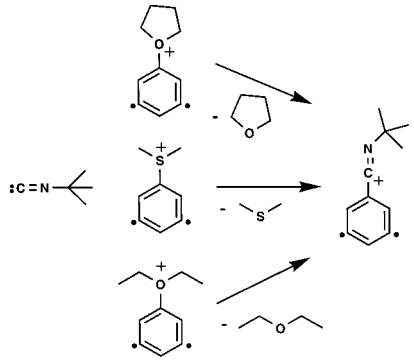

observed to undergo substitution as its sole reaction with *meta*-benzyne analogues with charged moieties of lesser basicity (Scheme 12). These substitutions of the less basic charge sites occur with higher efficiency than the CN-abstraction reactions with *meta*-benzyne analogues with more basic charge sites, indicating that addition to the *meta*-benzyne moiety is competitive on the time scale of the CN-abstraction reaction.

In fact, when the charge site is 3-fluoropyridine (rather than pyridine), substitution and CN-abstraction were both observed. On the basis of these observations, it is concluded to be likely that the initial CN-abstraction occurs via nucleophilic addition of *tert*-butyl isocyanide to the *meta*-benzyne moiety, followed by loss of the *tert*-butyl radical to result in a net-CN radical abstraction. The loss of *tert*-butyl radical can arise either by homolytic cleavage of the bond between the cyano-nitrogen and the *tert*-butyl group, or by a two-step process of heterolytic cleavage of this bond to form the *tert*-butyl cation followed by electron transfer between the two product fragments (Scheme 11).[57,58] This latter route has the additional virtue of helping to explain the other major reaction pathway, HCN abstraction. The HCN abstraction could result from the highly exothermic proton transfer (rather than electron transfer) between the *tert*-butyl cation and 3-pyridinium phenide intermediate. A similar addition−elimination mechanism can explain the CN-abstraction that is observed with benzyl isocyanide. However, HCN abstraction was not observed in this case. The absence of the HCN abstraction pathway can be explained by the drastic acidity differences between the benzyl and the *tert*-butyl cations, and is consistent with the general mechanism described above.

In many cases where charged *meta*-benzyne analogues display net-radical reactivity, this reactivity can be explained as a nucleophilic addition to the *meta*-benzyne moiety followed by fragmentation of the adduct. For example, dimethyl disulfide reacts with the *N*-(3,5-didehydrophenyl)pyridinium ion (**5**) by methylthio radical abstraction in a manner qualitatively similar to related phenyl radical analogues, albeit at significantly decreased reaction efficiencies (0.05% vs 8%, Table 3).

TABLE 3: Net-Radical Reactions of *Meta*-Benzyne Analogues Compared to Those of the Corresponding Phenyl Radical Analogues

meta-Benzyne Analog	Neutral reagent	Reaction[a]	Reaction Efficiency[b]	
			meta-benzyne[c]	phenyl radical[d]
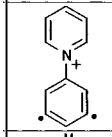	*tert*-Butyl isocyanide	CN-abstraction[e]	7%	20%
	Dimethyl disulfide	SCH_3-abstraction[f]	0.05%	8%[g]
	Iodine	I-abstraction	1.4%	18%
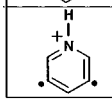	Dimethyl disulfide	SCH_3-abstraction[f]	53%	56%
	Allyl iodide	I-abstraction, allyl-abstraction	16%[h]	66%[g,i]

[a] Only reactions that are observed for both phenyl radical and *meta*-benzyne analogues are reported. [b] Reaction efficiency is defined as the ratio of the measured second-order reaction rate constant divided by the theoretical collision rate constant *x* 100. [c] The reaction efficiency takes into account only phenyl radical-type reaction pathways. [d] Matching phenyl radical reaction efficiencies are for the *N*-(3-dehydrophenyl)pyridinium and 3-dehydropyridinium cations. [e] This reaction makes up approximately one-third of the reactivity of the *meta*-benzyne analogue. The other reactivities include HCN abstraction and addition. [f] A minor product corresponding to $SSCH_3$ abstraction is also observed for the *meta*-benzyne analogue. [g] On the basis of the rate reported for the 3-fluoropyridinium analogue in Reference 49. [h] 60% I-abstraction and 40% allyl abstraction. [i] 90% I-abstraction and 10% allyl abstraction.

SCHEME 13

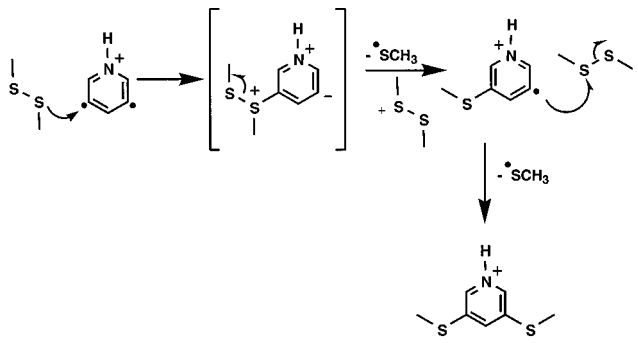

However, the same methylthio radical abstraction occurs for the 3,5-didehydropyridinium cation (**19**) at a reaction efficiency almost identical to that of its monoradical analogue, the 3-dehydropyridinium cation (53% vs 56% efficiency, respectively; Table 3). This latter example is particularly remarkable, as *the singlet ground state of this species*[59] *appears to have no retarding effect on the reaction.* It is clear that nucleophilic addition of dimethyl disulfide to the *meta*-benzyne moiety is taking place in the same time scale as the observed methylthio radical abstraction reactivity. The facility of nucleophilic addition by dimethyl disulfide is also apparent in the reactions of the 3,5-didehydrobenzoyl cation. Unlike the 3,5-didehydropyridinium cation, this species can undergo facile substitution if addition to the *meta*-benzyne moiety occurs. Rapid charge-site substitution (dimethyl disulfide for CO) is, in fact, what was observed for this species (Table 1), providing strong circumstantial evidence for the feasibility of a nucleophilic addition−fragmentation mechanism for the 3,5-didehydropyridinium ion as well. A mechanism similar to that of the above *tert*-butyl isocyanide case (Scheme 13) explains the methylthio abstraction reactivity without recourse to uncoupling of the biradical pair prior to or during reaction. It is believed that an analogous mechanism is responsible for the methylthio radical abstraction by the *N*-(3,5-didehydrophenyl)pyridinium ion (**5**). In this case, the large rate difference between *meta*-benzyne and phenyl radical analogues stems from two independent types

of reactivity whose rates are controlled by independent factors rather than a singlet ground-state perturbation of simple free-radical reactivity. Similar nucleophilic addition−fragmentation mechanisms also explain iodine atom abstraction from allyl iodide and molecular iodine (Table 3). In fact, such mechanisms should be suspected in any cases of apparent fast radical reactions by *meta*-benzynes with reagents of significant nucleophilicity.

Conclusions

The results presented for charged *meta*-benzyne analogues demonstrate that the *meta*-benzyne moiety is reactive toward nucleophiles. In the particular case of the charged analogues, this electrophilic reactivity is clearly observable in the charge-site substitution reactions that these species undergo. Despite the fact that the substitution reactivity only applies to a small subset of *meta*-benzyne analogues with good leaving groups, it provides great insight into the intrinsic reactivity of the *meta*-benzyne moiety. This is especially valuable in cases where fragmentation of the addition intermediate leads to net-radical reactions. The electrophilic addition−elimination mechanism proposed for these reactions have little conceptual similarity to the concerted radical reactions considered by Chen et al.[8] Thus, the apparent inconsistencies of these reactions with Chen's paradigm of singlet biradical reactions are resolvable by the simple realization that Chen's paradigm applies to radical reactions only. In this and other ways, the electrophilic reactivity reported herein represents a new and unexplored aspect of *meta*-benzyne reactivity.

The observation of this new reactivity also raises new questions to explore. Can *meta*-benzyne also act as a nucleophile? There is every reason to believe that it can. Of course, the positively charged *meta*-benzyne analogues used in this study cannot undergo charge-site substitution reactions with electrophiles; however, negatively charged species such as the 3,5-didehydrobenzoate anion might be able to. Does this electrophile/nucleophile reactivity have synthetic utility? Can the *para*-benzyne moiety also react as an electrophile, and if so, is such reactivity important in the pharmacological activity of the *para*-benzyne moiety toward DNA? It is hoped that further investigation into benzyne reactivity will help to address these and other questions.

Acknowledgment. This paper is dedicated to the memory of Prof. Robert R. Squires who carried out the first studies on charged *meta*-benzynes in the gas phase. Prof. Paul Wenthold is thanked for many helpful discussions. Prof. Veronica Bierbaum and Prof. Charles DePuy are thanked for the opportunity for experimentation on their SIFT-FA apparatus. Prof. Peter Armentrout and Prof. Kent Ervin are thanked for providing a modified version of the CRUNCH program. Dr. Shyam Karki is thanked for his insightful comparison of the electrophilic addition reactivity to the formation of carbene ylides. The National Science Foundation and the Purdue Research Foundation are acknowledged for financial support. The NCSA is thanked for the use of its computational resources.

References and Notes

(1) Wenthold, P. G.; Squires, R. R. *J. Am. Chem. Soc.* **1994**, *116*, 6401−6412.

(2) Wenthold, P. G.; Squires, R. R.; Lineberger, W. C. *J. Am. Chem. Soc.* **1998**, *120*, 5279−5290.

(3) (a) Marquardt, R.; Sander, W.; Kraka, E. *Angew. Chem.* **1996**, *35*, 746−748. (b) Sander, W.; Bucher, G.; Wandel, H.; Kraka, E.; Cremer, D.; Sheldrick, W. S. *J. Am. Chem. Soc.* **1997**, *119*, 10 660−10 672. (c) Sander, W.; Exner, M. *Perkin Trans. 2* **1999**, 2285−2290.

(4) Raghavachari, K.; Trucks, G. W.; Pople, J. A.; Head-Gorden, M. *Chem. Phys. Lett.* **1989**, *157*, 479−483.

(5) Sander, W. *Acc. Chem. Res.* **1999**, *32*, 669−676.

(6) Hu, J.; Squires, R. R. *J. Am. Chem. Soc.* **1996**, *118*, 5816−5817.

(7) Thoen, K. K.; Kenttämaa, H. I. *J. Am. Chem. Soc.* **1999**, *121*, 800−805.

(8) Logan, C. F.; Chen, P. *J. Am. Chem. Soc.* **1996**, *118*, 2113-2114.

(9) Schottelius, M. J.; Chen, P. *J. Am. Chem. Soc.* **1996**, *118*, 4896−4903.

(10) Roth, W. R.; Hopf, H.; Wasser, T.; Zimmermann, H.; Werner, C. *Liebigs Ann.* **1996**, 1691−1695.

(11) The "uncoupling" of the singlet electron pair concerted with reaction can take the form of a transition from closed-shell singlet to open-shell singlet during the course of the reaction. This would produce the same net effect as intersystem crossing (i.e., allowing radical reactions) while conserving spin. The calculations of Reference 8 find singlet transition states for *para*-benzyne hydrogen atom abstraction that may imply such an open shelled singlet electronic structure.

(12) Chen, P. *Angew. Chem.* **1996**, *35*, 1478−1480.

(13) Nelson, E. D.; Artau, A.; Price, J. P.; Tichy, S. E.; Kenttämaa, H. I. *J. Am. Chem. Soc.* **2000**, *122*, 8781−8782.

(14) Gord, J. R.; Freiser, B. S. *Anaytica Chimica Acta* **1989**, *225*, 11−24.

(15) (a) Schweikhard, L.; Guan, S.; Marshall, A. G. *Int. J. Mass Spectrom. Ion Processes* **1992**, *120*, 71−83. (b) Guan, S.; Xiang, X.; Marshall, A. G. *Int. J. Mass Spectrom. Ion Processes* **1993**, *124*, 53−67.

(16) (a) Thoen, K. K.; Kenttämaa, H. I. *J. Am. Chem. Soc.* **1997**, *119*, 3832−3833. (b) Smith, R. L.; Kenttämaa, H. I. *J. Am. Chem. Soc.* **1995**, *117*, 1393−1396. (c) Thoen, K. K.; Smith, R. L.; Nousiainen, J. J.; Nelson, E. D.; Kenttämaa, H. I. *J. Am. Chem. Soc.* **1996**, *118*, 8669−8676.

(17) The sustained off-resonance irradiation for collision-activated dissociation (SORI−CAD) method was employed using an argon or helium target gas that was pulsed into the cell at a peak pressure of $\sim 10^{-5}$ Torr. For details of this method, see: Gauthier, J. W.; Trautman, T. R.; Jacobson, D. B. *Analytica Chimica Acta* **1991**, *246*, 211−245.

(18) The carbon−bromine bond is sufficiently strong that an attempt to cleave bromine substituents with CAD can result in ion isomerization. For this reason, bromine substituents were only used to generate the second of the two *meta*-benzyne radical sites. The formation of the *meta*-benzyne moiety reduces the bond strength by ~20 kcal/mol (see for example Blush et al. *Acc. Chem. Res.* **1992**, *25*, 385−392.), alleviating concerns of isomerization.

(19) The dissipation of internal energy through IR emission by ions trapped in an FT-ICR has been shown to be quite rapid compared to the time scale of the present experiment. For more information on studies of IR emission rates by trapped ions see Dunbar, R. C. *Mass Spectrom. Rev.* **1992**, *11*, 309−339.

(20) Wang, T. C. L.; Rica, T. L. Marshall, A. G. *Anal. Chem.* **1986**, *58*, 2938.

(21) (a) Su, T.; Chesnavich, W. J. *J. Chem. Phys.* **1982**, *76*, 5183−5185. (b) Chesnavich, W. J.; Su, T.; Bowers, M. T. *J. Chem. Phys.* **1980**, *72*, 2641−55.

(22) Leek, D. T.; Stirk, K. M.; Zeller, L. C.; Kiminkinen, L. K. M.; Castro, L. M.; Vainiotalo, P.; Kenttämaa, H. I. *J. Am. Chem. Soc.* **1994**, *116*, 3028.

(23) Marinelli, P. J.; Paulino, J. A.; Sunderlin, L. S.; Wenthold, P. G.; Poutsma, J. C.; Squires, R. R. *Int. J. Mass Spectrom. Ion Processes* **1994**, *130*, 89−105.

(24) Nelson, E. D.; Kenttämaa, H. I. *J. Am. Soc. Mass Spectrom.* **2001**, *12*, 258−267.

(25) Sunderlin, L. S.; Wang, D.; Squires, R. R. *J. Am. Chem. Soc.* **1993**, *115*, 12 060.

(26) (a) Ervin, K. M.; Loh, S. K.; Aristov, N.; Armentrout, P. B. *J. Phys. Chem.* **1989**, *87*, 3593. (b) Ervin, K. M.; Armentrout, P. B. *J. Phys. Chem.* **1985**, *83*, 166−189.

(27) Schultz, R. H.; Crellin, K. C.; Armentrout, P. B. *J. Am. Chem. Soc.* **1991**, *113*, 8590.

(28) (a) Schultz, R. H.; Crellin, K. C.; Armentrout, P. B. *J. Am. Chem. Soc.* **1991**, *113*, 8590. (b) Rodgers, M. T.; Ervin, K. M.; Armentrout, P. B. *J. Chem. Phys.* **1997**, *106*, 4499.

(29) Chantry, P. J. *J. Chem. Phys.* **1971**, *55*, 2746.

(30) Frisch, M. J.; Trucks, G. W.; Schlegel, H. B.; Scuseria, G. E.; Robb, M. A.; Cheeseman, J. R.; Zakrzewski, V. G.; Montgomery, J. A. Jr.; Stratmann, R. E.; Burant, J. C.; Dapprich, S.; Millam, J. M.; Daniels, A. D.; Kudin, K. N.; Strain, M. C.; Farkas, O.; Tomasi, J.; Barone, V.; Cossi, M.; Cammi, R.; Mennucci, B.; Pomelli, C.; Adamo, C.; Clifford, S.; Ochterski, J.; Petersson, G. A.; Ayala, P. Y.; Cui, Q.; Morokuma, K.; Malick, D. K.; Rabuck, A. D.; Raghavachari, K.; Foresman, J. B.; Cioslowski, J.; Ortiz, J. V.; Baboul, A. G.; Stefanov, B. B.; Liu, G.; Liashenko, A.; Piskorz, P.; Komaromi, I.; Gomperts, R.; Martin, R. L.; Fox, D. J.; Keith, T.; Al-Laham, M. A.; Peng, C. Y.; Nanayakkara, A.; Gonzalez, C.; Challacombe,

M.; Gill, P. M. W.; Johnson, B.; Chen, W.; Wong, M. W.; Andres, J. L.; Gonzalez, C.; Head-Gordon, M.; Replogle, E. S.; Pople, J. A. *Gaussian 98*, Revision *A.7*; Gaussian, Inc.: Pittsburgh, PA, 1998.

(31) Schaftenaar, G.; Noordik, J. H. *J. Comput.-Aided Mol. Design* **2000**, *14*, 123−134.

(32) Lias, S. G.; Bartmess, J. E.; Liebman, J. F.; Holmes, J. L.; Levin, R. D.; Mallard, W. G. Ion Energetics Data In *the NISTChemistry WebBook, NIST Standard Reference Database Number 69*; Mallard, W. G., Linstrom, P. J., Eds.; National Institute of Standards and Technology: Gaithersburg, MD, February, 2000, 20 899 (*http://webbook.nist.gov*).

(33) This is characteristic of gas-phase ion−molecule reactions. See for example, Brauman, J. I. *J. Mass Spectrom.* **1995**, *30*, 1649−1651.

(34) This dipole moment was estimated by single point calculations at the MP2/6-31+G(d) level of theory. In comparison, two Li^+ and F^- placed at the same relative positions as the centers of formal charge in the intermediate have a 21 D dipole moment at the same level of theory. Calculations at the HF/6-31+G(d) level of theory also predict a 9.8 D dipole moment for **9**. However, density functional theory calculations predict a significantly lower value. For example, BLYP/6-31+G(d) calculations predict a dipole moment of only 2.38 D.

(35) (a) Campbell, S.; Rodgers, M. T.; Marzluff, E. M.; Beauchamp, J. L. *J. Am. Chem. Soc.* **1994**, *116*, 9765−9766. (b) Campbell, S.; Rodgers, M. T.; Marzluff, E. M.; Beauchamp, J. L. *J. Am. Chem. Soc.* **1995**, *117*, 12 840−12 854.

(36) (a) Freitas, M. A.; Marshall, A. G. *Int. J. Mass Spectrom.* **1999**, *183*, 221−231. (b) Jockusch, R. A.; Price, W. D.; Williams, E. R. *J. Phys. Chem. A* **1999**, *103*, 9266−9274.

(37) (a) Broadus, K. M.; Kass, S. R. *J. Am. Chem. Soc.* **2000**, *122*, 9014−9018. (b) Wang, X. B.; Broadus, K. M.; Wang, L. S.; Kass, S. R. *J. Am. Chem. Soc.* **2000**, *122*, 8305−8306.

(38) Padwa, A.; Hornbuckle, S. F. *Chem. Rev.* **1991**, *91*, 263−309, and references therein.

(39) This estimate is based on the covalent bonding of **9** and its predicted 30 kcal/mol dissociation energy. Similar (and even much greater) lifetimes have been observed and theoretically predicted for covalently bound ion-molecule adducts. See for example: (a) Anicich, V. G.; Sen, A. D.; Huntress, W. T. Jr.; McEwan, M. J. *J. Chem. Phys.* **1991**, *94*, 4189−91. (b) Anicich, V. G.; Sen, A. D.; McEwan, M. J.; Smith, S. C. *J. Chem. Phys.* **1994**, *100*, 5696−705.

(40) Based on the collision rate predictions of the method of Reference 21.

(41) This reaction was carried out in the central quadrupole rather than the flow tube to avoid confusion from an isomeric contaminant corresponding to an electrostatic cluster of the 4-*tert*-butylpyridinium trifluoroborate zwitterion and the *N*-(3,5-didehydrophenyl)-4-*tert*-butylpyridinium ion.

(42) (a) Hill, B. T.; Poutsma, J. C.; Chyall, L. J.; Hu, J.; Squires, R. R. *J. Am. Soc. Mass Spectrom.* **1999**, *10*, 896−906. (b) Wenthold, P. G.; Hu, J.; Squires, R. R. *J. Am. Chem. Soc.* **1996**, *118*, 11 865−11 871.

(43) The efficiency of this reaction was measured using pyridine-d_5 as (alternately) the nucleophile or leaving group. The efficiencies measured in both cases agree to within the experimental error.

(44) MP2/6-31+G(d) calculations of a Li_2F^+ model system in which Li^+ and F^- ions were placed at relative orientations corresponding to the centers of formal charge in the 3,5-bis(pyridinium)phenide intermediate suggest that this intermediate possesses approximately half (24 kcal/mol) of the ion−dipole stabilization energy of the salt bridged species with a relaxed geometry (i.e., 180° Li−F−Li angle).

(45) Shaik, S.; Shurki, A. *Angew. Chem., Int. Ed.* **1999**, *38*, 586−625, and references therein.

(46) The phenyl cation provides an approximation of the zwitterionic valence state of *meta*-benzyne. Addition of pyridine to the cationic moiety is a barrierless bond formation process.

(47) Neon serves as an approximation of the size and electrostatic effect of a nitrogen atom. The biradical electron pair of *meta*-benzyne is polarized by electrostatic repulsion from the neon electron cloud without the formation of a chemical bond.

(48) The reverse of this reaction, CAD of 3-chlorophenide to form chloride and *meta*-benzyne, was used to measure the heat of formation of *meta*-benzyne by Wenthold et al. (Reference 1) and appears to be in good agreement with high-level theoretical calculations (Cramer, et al. *Chem. Phys. Lett*. **1997**, *277*, 311−320 and references therein).

(49) (a) Heidbrink, J. L.; Thoen, K. K.; Kenttämaa, H. I. *J. Org. Chem.* **2000**, *65*, 645−651. (b) Tichy, S. E.; Thoen, K. K.; Price, J. M.; Ferra, J. J., Jr.; Petucci, C. J.; Kenttämaa, H. I. *J. Org. Chem*. **2001**, *66*, 2726−2733.

(50) See for example: (a) Jones, M., Jr.; Levin, R. H. *J. Am. Chem. Soc.* **1969**, *91*, 6411−6415. (b) Atkin, R. W.; Rees, C. W. *Chem. Commun.* **1969**, 152. (c) Hatch, L. F.; Peter, D. *Chem. Commun.* **1968**, 1499. (d) Huebner, C. F.; Donoghue, E. M. *J. Org. Chem.* **1968**, *33*, 1678−9. (e) Wittig, G. *Angew. Chem., Internat. Edit.* **1965**, *4*, 731−737.

(51) (a) Nakayama, J.; Akimoto, K. *Sulfur Rep*. **1994**, *16*, 61−111. (b) Hayes, D. M.; Hoffmann, R. *J. Phys. Chem.* **1972**, *76*, 656−663. (c) Tabushi, I.; Okazaki, K.; Oda, R. *Tett. Lett.* **1967**, 3591−3593.

(52) Based on BLYP/6-31+G(d) calculations of the nonfluorosubstituted analogues.

(53) Such species may, however, be subject to substitution by electrophiles, and further research will address this possibility.

(54) Kim, S. S.; Yang, K. W.; Lee, C. S. *J. Org. Chem.* **1996**, *61*, 4827−4829.

(55) It is assumed that the charged moiety has no profound effect on the singlet−triplet gap of the *meta*-benzyne moiety. This is consistent with recent computational studies (Cramer, C. J. *J. Am. Chem. Soc.* **1998**, *120*, 6261−6269. Cramer, C. J.; Debbert, S. *Chem. Phys. Lett.* **1998**, *287*, 320−326.) that predict that didehydropyridinium ions possess singlet-triplet gaps only slightly perturbed from that of the analogous benzyne. We have confirmed this for the species discussed in this paper by using the hyperfine coupling method of Cramer, et al. (*J. Phys. Chem*. A **1997**, *101*, 9191−9194.).

(56) The double-well potential energy surface characteristic of ion−molecule reactions can often result in the transition state lying below the reactants in energy (e.g., Figure 2). In effect, the thermal energy of the system is augmented by electrostatic ion−molecule solvation energy that helps to overcome the chemical barrier. This can often result in faster reactions than are observed for neutral species. However, the relative reaction rates of ion−molecule reactions are affected by perturbations in the barrier height in a manner roughly analogous to neutral species (i.e., directly proportional to the ratio of the sums of states above each transition state). See for example: (a) Olmsteadm, W. N.; Brauman, J. I. *J. Am. Chem. Soc.* **1977**, *99*, 4219−4228. (b) Wilbur, J. L.; Wladkowski, B. D.; Brauman, J. I. *J. Am. Chem. Soc.* **1993**, *115*, 10 823−10 829.

(57) This sort of two-step reaction has been observed previously with *tert*-butyl isocyanide. See for example: (a) Nelson, E. D.; Li, R.; Kenttämaa, H. I. *Int. J. Mass Spectrom.* **1998**, *185/186/187*, 91−96. (b) Nelson, E. D.; Thoen, K. K.; Kenttämaa, H. I. *J. Am. Chem. Soc.* **1998**, *120*, 3792−3798.

(58) Homolytic dissociation is estimated to be ∼40 kcal/mol more exothermic than heterolytic dissociation based on IE and EA values from References 32 and 54. However, homolytic dissociation is presumably accompanied by a barrier, and it is unclear whether a direct or two-step process takes place.

(59) Cramer, C. J.; Debbert, S. *Chem. Phys. Lett.* **1998**, *287*, 320−326.